

# RF Coil Element with Longitudinal and Transversal Two-Peak Field Distribution for Low SAR 7-Tesla Magnetic Resonance Imaging

Zhichao Chen<sup>1,2</sup>, Klaus Solbach<sup>2</sup>, Daniel Erni<sup>1</sup>, and Andreas Rennings<sup>1</sup>

<sup>1</sup> General and Theoretical Electrical Engineering (ATE), Faculty of Engineering, University of Duisburg-Essen and CENIDE – Center for Nanointegration Duisburg Essen, D-47048 Duisburg, Germany

<sup>2</sup> High Frequency Engineering (HFT), Faculty of Engineering, University of Duisburg-Essen, D-47048 Duisburg, Germany

**Abstract**—In ultra high field MRI ( $B_0 \geq 7$  T) the allowed local SAR restricts the power that can be applied to the RF coil. Here in this paper we propose an approach where the power that is absorbed by the body is better distributed, yielding a lower  $SAR_{max}$  value, hence higher power level can be used for feeding. The optimized SAR distribution is excited by an extended dipole (41 cm-long), which is longer than the ordinary half-wavelength one, and an eigen-resonant metal plate used for shielding purpose. At 300 MHz, the excited dipole has an approximate  $3\lambda/2$  electrical length where the maximum of current is located away from the feeding position, exciting a longitudinal two-peak SAR distribution, whereas the passive shielding plate exhibits a half-wavelength eigen-resonance, which yields a transversal two-peak SAR distribution. Compared to an established strip line element (25 cm-long), a 29% improvement of figure of merit ( $H_{mean}/\sqrt{SAR_{max}}$ ) is obtained based on simulation.

**Index Terms**—Low SAR; RF coil; 7-T MRI; two-peak distribution.

## I. INTRODUCTION

Multi-channel RF coils based on several longitudinally oriented strip line elements have been successfully applied in ultra-high field MRI. Among the different utilized dipole approaches [1], [2], [3], the symmetrically fed RF coil element which was terminated by two meanders [2] seems to be one of the most promising candidates. This 25 cm-long element with meanders has been used, e.g., to scan the first homogeneous “from top to toe” MR image at 7 T [4]. In [5] an extended version with longitudinal two-peak SAR distribution was proposed. In both versions [2], [5] the meanders were connected to an adjacent metal plate (2 cm away from the coil) by using a so-called end-capacitor in order to control the current distribution along the strip line.

Here in this paper another 41 cm-long strip line coil with different coupling to the shielding plate is proposed. Instead of the direct lumped-element-connection between meanders and metal plate a field-based coupling is used, which enables the plate to resonate in its natural half-wavelength eigen-mode. The resonant current on the shielding plate, together with the excitation current in the strip line produces longitudinally and transversally two-peak electric and magnetic field distributions above the coil element where the body is located.

## II. RF COIL WITH DIFFERENT COUPLING STRATEGIES

The strip line elements with different coupling strategies are depicted in Fig. 1. The strip line element and the corresponding

shielding plate are printed on Rogers RO4003 substrates ( $\epsilon_r = 3.55$ ) with a thickness of 0.5 mm, which are separated by 19 mm of air. The width of the strip line and the shielding plate are set to 1.5 cm and 10 cm, respectively. The geometry of the meanders remains unchanged in comparison to [2], but here we add high-dielectric material for the novel design in order to increase the electrical length of the meander. Specifically, the thickness of the high-dielectric substrates above and beneath the meanders are set to 1.5 mm and 3 mm, respectively.

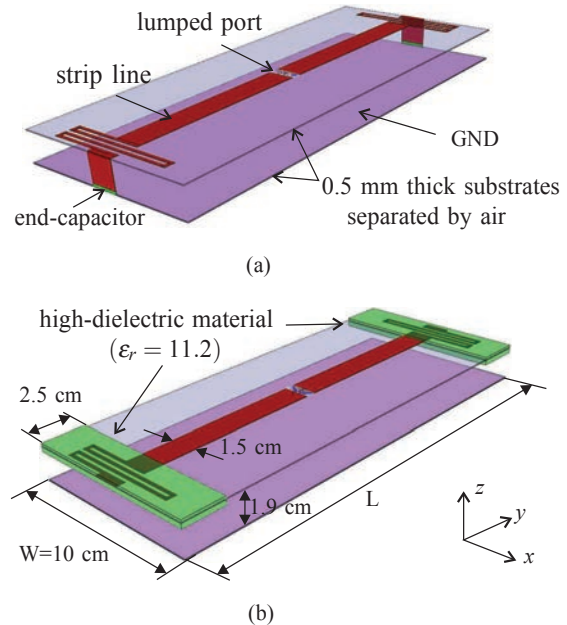


Fig. 1. RF coil elements with different coupling strategies: (a) strong coupling via lumped end-capacitor (established design), (b) field-based coupling with distributed high-dielectric substrates (novel design).

## III. TWO-PEAK FIELD DISTRIBUTION

For the MRI applications a local  $SAR_{max}$  inside the human body should be minimized. Meanwhile, a uniform magnetic field distribution inside a broad field of view (FoV) is desirable. The performance of the RF coil can be evaluated by the figure of merit (FoM), here defined as:

$$FoM = \frac{\text{mean}(|\vec{H}|)}{\sqrt{\text{max}(SAR)}} \quad (1)$$

where

$$SAR \propto |\vec{E}|^2. \quad (2)$$

Here we compare the proposed novel design with the established one. The comparison is carried out based on full-wave FDTD simulation and measurements.

### A. Full-wave Simulation

The 25 cm-long and 41 cm-long coil elements are simulated together with a flat phantom ( $\epsilon_r = 45.3$ ,  $\delta = 0.87$  S/m) which is separated 2 cm from the top PCB by air at 300 MHz. In order to evaluate the field distribution of the aforementioned coil elements, we define an area 3 cm inside that phantom in xy-plane with the same dimension as the coil element ( $W \times L$ ). The magnetic and electric field distribution on the pre-defined evaluation area extracted from full-wave simulation are shown in Fig. 2(a)-(d). Since the excited electro-magnetic field is closely related to the current on the strip line as well as the corresponding shielding plate, the current distribution on the strip line as well as on the corresponding shielding plate are of our interest and given in Fig. 2(e)-(f).

For the 25 cm-long version, it can be seen from Fig. 2(e) that a direct mirror current is concentrated in the vicinity of the longitudinal axis on the shielding plate. Consequently, the maximum of electric and magnetic fields are located on the longitudinal axis as shown in Fig. 2(a) and Fig. 2(c).

For the element with eigen-resonant shielding plate, similar to the previous case, a direct mirror current can be found on the shielding plate under the strip line. Additional to this current, due to the loose field-based coupling, the shielding plate exhibits a half-wavelength eigen-resonance with a length of 41 cm, producing eigen-resonant currents along the longitudinal edges as shown in Fig. 2(f). This resonant current results in a special two-peak distribution of electric and magnetic fields in the transversal direction. Meanwhile, the strip line element exhibits a two-peak electric and magnetic field distribution in the longitudinal direction due to a longer extent, which has been revealed in [5] as well. These two effects adding together, as shown in Fig. 2(b) and Fig. 2(d), the maximum of total electric field is shifted to the outer district of the evaluation area in comparison to the 25 cm element. As a drawback, the total magnetic field is reduced, however, with a better homogeneity and a broader FoV. Nevertheless, a 29% improvement on FoM based on the calculated field parameters which are given in Tab. I is obtained.

TABLE I  
FDTD SIMULATION RESULTS

Coil	$H_{\text{mean}}$ (A/m)	$E_{\text{max}}$ (V/m)	$\frac{H_{\text{mean}}}{E_{\text{max}}}$ (A/V)	Improvement on FoM
25 cm-long	0.150	13.68	0.011	29%
41 cm-long	0.084	5.89	0.0142	

In order to verify the eigen-resonance of the shielding plate, a metal plate with the dimension of 41 cm $\times$ 10 cm is excited by a normal incident plane wave. The overall current flowing through the cross section of the plate is integrated versus

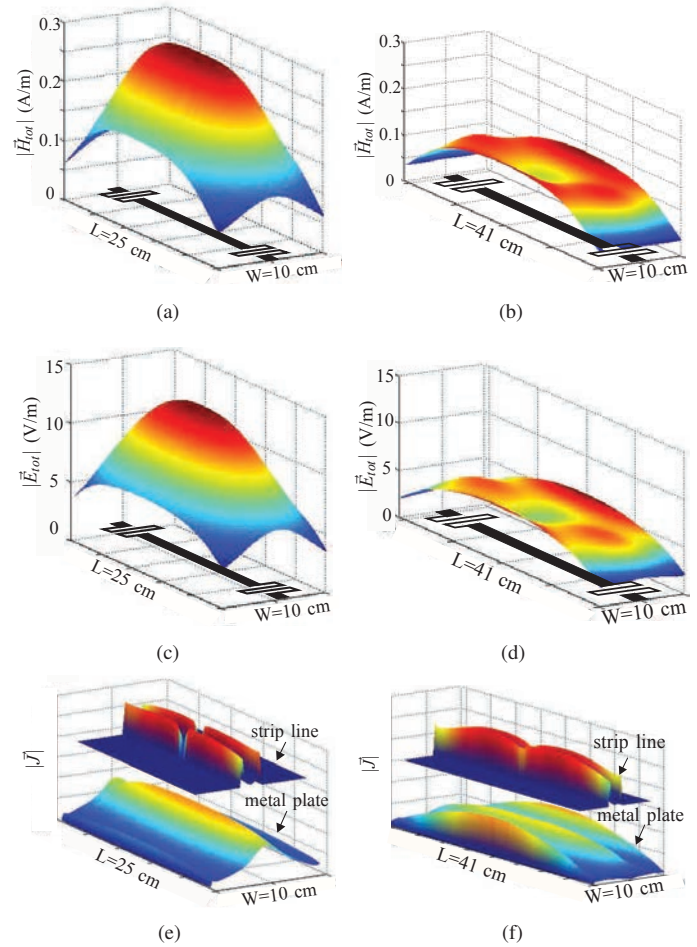


Fig. 2. FDTD simulation results: (left) 25 cm-long coil and (right) 41 cm-long coil. (a) (b) Magnetic field distribution and (c) (d) electric field distribution on the plane which is 3 cm inside the phantom (5 cm away from the top PCB). The  $|\vec{H}_{\text{tot}}|$  and  $|\vec{E}_{\text{tot}}|$  refer to the absolute values of the total magnetic and electric fields in the case of the accepted power of the coil element is equal to 1 W, respectively. (e) (f) The current density on the strip line and the corresponding shielding plate.

frequency. From the current distribution in Fig. 3(a) and the current-frequency curve in Fig. 3(b) we can conclude that the metal plate exhibits a half-wavelength resonance at 300 MHz and the resonant current is concentrated in the vicinity of the longitudinal edge of the metal plate.

### B. Prototypes and Measurement

The prototypes of the strip line elements to be compared are shown in Fig. 4, the one with shorter extent in Fig. 4(a) is loaded with end-capacitor and the longer one in Fig. 4(b) is loaded with distributed high-dielectric substrates, here Rogers RO3010 ( $\epsilon_r = 11.2$ ). The matching network for the both elements are with the same topology except the values of the used chip capacitors. The matching network consists of a pair of shunt capacitors with fixed values and a tunable series capacitor. Additionally, a balun with 180° delay coaxial cable is employed here [1]. With the appropriately chosen values of the shunt and series capacitors, a more than 16 dB return

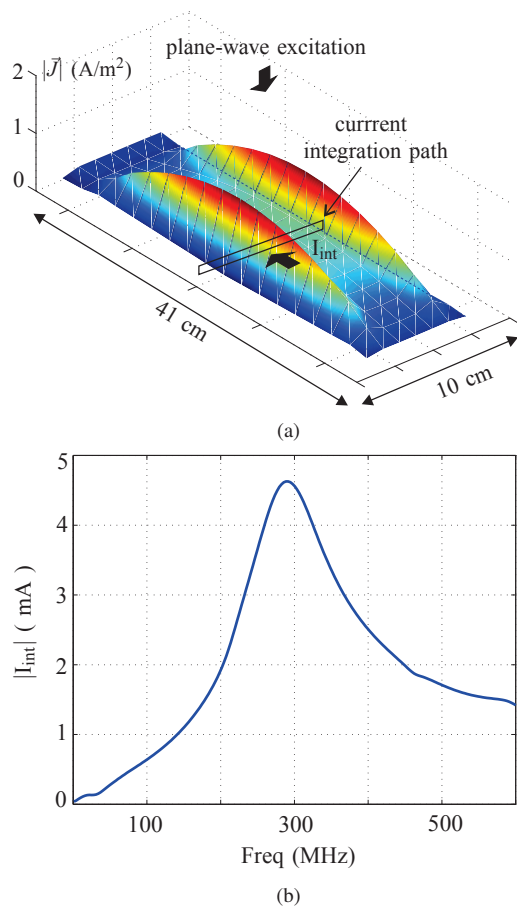


Fig. 3. Eigen-resonance behavior of a 41 cm×10 cm metal plate. (a) 2D current distribution on the metal plate at 300 MHz and (b) the overall current flowing through the cross section of the plate versus frequency.

loss can be achieved for the both cases. The input power is set to 20 W, considering the sufficient matching for the both elements, the accepted power is basically the same, hence the comparison of the measured fields is carried out in a fair manner.

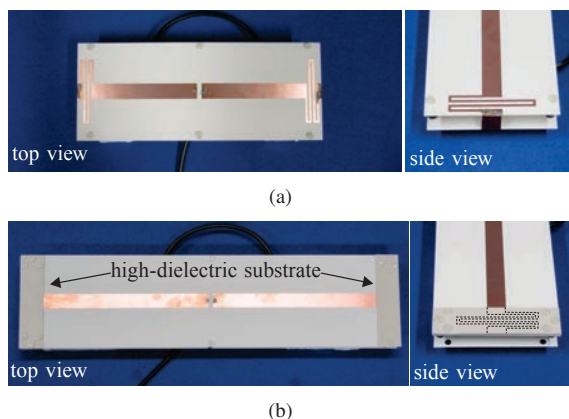


Fig. 4. Front- and side view of the prototypes of (a) 25 cm-long and (b) 41 cm-long coil elements.

The measurement setup is shown in Fig. 5. The field probe for electric/magnetic field measurement is driven by a positioning system, which is connected to the control unit. In order to emulate the human body in the frequency range around 300 MHz, a polyamide container is filled with fluid ( $\epsilon_r \approx 45.3$ ,  $\delta \approx 0.87$  S/m) and placed 2 cm above the coil element. The magnitude of the total electric and magnetic fields inside that phantom (5 cm above the top PCB) are measured and plotted in Fig. 6. The blue and red curves indicate the measured electric/magnetic field in longitudinal and transversal directions, respectively.

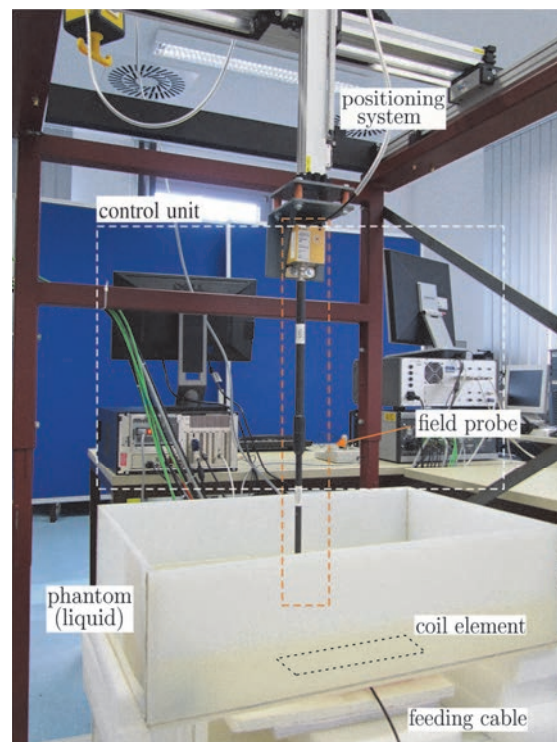


Fig. 5. The experimental setup for the near-field (electric and magnetic) measurement.

It can be seen from Fig. 6 and Fig. 2 that the measured electric and magnetic field distributions show a good agreement with the simulated results. In general, the measured results are smaller than the simulated ones, this might be caused by the deviation of the phantom parameter and the imprecise alignment of the experimental setup. For the 25 cm version, as we expected, the maximum of the electric and magnetic fields of the transversal scans are located on the longitudinal axis of the coil element, while the longitudinal scans indicate that the electric and magnetic fields are quite uniform in the center range and decay rapidly as reach the meander sections. For the 41 cm version, the maximum of electric and magnetic fields on the transversal cuts are shifted away from the center of the FoV. The longitudinal scans on the edges of the FoV exhibit a maximum in the center according to the resonant current on the shielding plate, while the scan across longitudinal axis shows a two-peak distribution due to the longer extent.

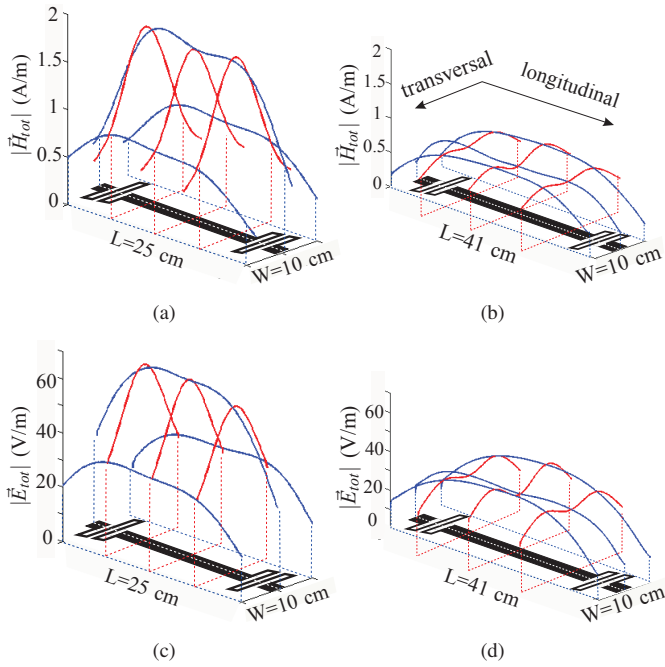


Fig. 6. Measured results: (left) 25 cm-long coil and (right) 41 cm-long coil. The magnitude of (a) (b) magnetic field and (c) (d) electric field inside phantom (5 cm above the top PCB) in longitudinal and transversal directions.

#### IV. CONCLUSION

RF coil elements with diverse coupling strategies have been presented. The performance of the 25 cm-long established coil and the proposed 41 cm-long coil is investigated and compared. Since the meandered end sections of the 41 cm-long version are not directly connected to the shielding plate, the plate exhibits a half-wavelength resonance, producing resonant currents located on the longitudinal edges of the plate, which results in a two-peak distribution of the electric and magnetic fields in the transversal direction above the coil. Additionally, a two-peak distribution in longitudinal direction is achieved due to the longer extent of the strip line. Compare to the 25 cm-long version, the total electric field is significantly reduced and a local minimum is obtained in the center area of the FoV. As a drawback, the total magnetic field is reduced as well, however, with better a homogeneity and a broader FoV. A 29% improvement of figure of merit ( $H_{\text{mean}}/\sqrt{SAR_{\text{max}}}$ ) is obtained based on simulation. The proposed approach to diminish the total electric field with two-peak distribution has been fully confirmed by full-wave simulation and experimental results.

There are also some further investigations required in the future. Due to the lower  $SAR_{\text{max}}$  value, the 41 cm-long coil element is supposed to be capable of a higher input power, the magnetic and electric field distribution in such a high power level will be investigated. Another issue we will focus on is the coupling of the novel 41 cm-long coil elements in a multi-channel MRI scanner.

#### ACKNOWLEDGMENT

This work has been supported by the German Science Foundation (DFG).

#### REFERENCES

- [1] D. O. Brunner, N. De Zanche, J. Froehlich, D. Baumann, and K. Pruessmann, "A symmetrically fed microstrip coil array for 7T," in *15th Proc. Intl. Soc. MRM*, p. 448, 2007.
- [2] S. Orzada, A. Bahr, and T. Bolz, "A novel 7 T microstrip element using meanders to enhance decoupling," in *16th Proc. Intl. Soc. MRM*, p. 2979, 2008.
- [3] A. J. E. Raaijmakers, O. Ipek, D. W. J. Klomp, C. Possanzini, P. R. Harvey, J. J. W. Lagendijk, and C. A. T. van den Berg, "Design of a Radiative Surface Coil Array Element at 7 T: The Single-Side Adapted Dipole Antenna," *Magnetic Resonance in Medicine (MRM)*, vol. 66, pp. 1488–1497, 2011.
- [4] S. Orzada, S. Maderwald, O. Kraff, I. Brote, M. E. Ladd, K. Solbach, P. Yazdanbakhsh, A. Bahr, H. P. Fautz, and A. K. Bitz, "16-Channel Tx/Rx Body Coil for RF Shimming with Selected Cp Modes at 7T," in *18th Proc. Intl. Soc. MRM*, p. 50, 2010.
- [5] A. Rennings, A. Litinsky, P. Schneider, S. Orzada, and S. Otto, "Full-Wavelength Dipole RF Coil Element for 7 T MRI with Maximized Longitudinal FOV and Two-Peak SAR Distribution," in *19th Proc. Intl. Soc. MRM*, p. 3813, 2011.